energies

MDPI

Article

Online Estimation of the Mechanical Parameters of a Wind Turbine with Doubly Fed Induction Generator by Utilizing Turbulence Excitations

Yening Lai [1], Ling Zhu [1], Xueping Pan [2,*], Jinpeng Guo [2], Dazhuang He [2] and Wei Liang [2]

[1] NARI Group Corporation (State Grid Electric Power Research Institute), Nanjing 211100, China; laiyening@sgepri.sgcc.com.cn (Y.L.); zhuling@sgepri.sgcc.com.cn (L.Z.)
[2] College of Energy and Electrical Engineering, Hohai University, Nanjing 211100, China; jinpeng.guo@mail.mcgill.ca (J.G.); dazhuag_he@hhu.edu.cn (D.H.); 190206030005@hhu.edu.cn (W.L.)
* Correspondence: xueping_pan@hhu.edu.cn

Abstract: In this paper, a new method using wind turbulence excitation is proposed to estimate the parameters of the mechanical system (drivetrain and pitch angle controller) in a Doubly Fed Induction Generator (DFIG) Wind Turbine (WT). Firstly, simulations were carried out for a DFIG WT under turbulence excitations. The spectral contents of the responses imply that the transients of the electrical system (generator and converter), which are much faster than those of the mechanical system, can be neglected when estimating the mechanical parameters. Based on this, a simplified model related to the mechanical system of the DFIG WT was derived by applying the model reduction technique. Secondly, the parameter sensitivity of Power Spectral Density (PSD) was used to quantify the impacts of individual parameters on the dynamics of the mechanical system, and the influential parameters were selected on the basis of the sensitivity results. Finally, a weighted least-squares optimization problem, which is suitable for a system with close oscillation modes, was formulated for parameter estimation. The estimation results based on two different types of optimization methods were compared, and their estimation accuracies validate the effectiveness of the proposed method.

Keywords: DFIG; identifiability; parameter estimation; PSD sensitivity; weighted Levenberg–Marquardt method

Citation: Lai, Y.; Zhu, L.; Pan, X.; Guo, J.; He, D.; Liang, W. Online Estimation of the Mechanical Parameters of a Wind Turbine with Doubly Fed Induction Generator by Utilizing Turbulence Excitations. *Energies* **2022**, *15*, 2277. https://doi.org/10.3390/en15062277

Academic Editors: Albert Smalcerz and Marcin Blachnik

Received: 8 February 2022
Accepted: 18 March 2022
Published: 21 March 2022

1. Introduction

Wind turbine technology has experienced rapid developments in the past few years. A DFIG WT can be operated over a wide range of rotor speeds and therefore is considered one of the most popular technologies to generate power from wind. To achieve its full potential, accurate representation of the DFIG WT is of vital importance. Detailed or generic models have been developed in many papers [1,2]. However, it is a common practice to use either "manufacturer specified" or "typical" values to specify the WT's parameters, which may lead to significant inaccuracy because many parameters or operating conditions may change over time. In this context, there are efforts to develop online estimation methods for obtaining the parameters of a WT [3].

Testing the design is an important task for parameter estimation since one test can only excite partial dynamics of the system, and the parameters corresponding to the excited dynamics can be estimated. Normally, disturbances in the power grid, such as voltage dips or short-circuit faults, are applied, and power measurements are used to validate models of wind turbines [4–9]. In [10], an experiment to estimate the mechanical parameters of WTs was performed by islanding the wind farm. In [11–13], a short-circuit fault was used to estimate the inertia of a WT based on measurements of frequency trajectories, and in [14], the parameters of an induction generator were identified based on the change in system frequency. In [15], to overcome the disadvantage of the model reference adaptive system method of needing to excite all of the system dynamics, a new online estimation method that does not require an excitation signal was investigated to estimate DFIG parameters. However, many tests can only be performed by manufacturers, and post-disturbance data may be insufficient in real cases, introducing more challenges when conducting parameter estimations. A parameter estimation procedure can be formulated as an optimization problem, and the optimization objective is to determine parameter values by curve fitting techniques. In [16], a recursive least-squares algorithm was applied, and the estimation results showed that the algorithm was able to track the actual values of parameters with rapid variations. In Reference [5], the cubature Kalman filter, which can be used to estimate both the system dynamic state and a modified set of parameters, was proposed for variable-speed permanent magnet synchronous machine wind turbines, and the robustness of the technique was proven with three different performance tests.

In recent years, with the development of artificial intelligence and wide-area measurement technology, data-driven methods for WT modeling have been developed. In Reference [17], a neural network–based nonlinear wind turbine model was proposed to estimate the output power of a wind turbine, and a real example showed that the estimated mean square errors were less than 1%. In [18], a deep auto-encoder network based on SCADA data combined with extreme value theory was applied to determine the fault components of wind turbines. Reference [19] proposed a dynamic load modeling method based on a long short-term memory neural network. Data-driven methods are highly adaptable when the model structure is unknown or difficult to express mathematically. However, they typically require a large amount of historical data, and the model accuracy can be easily affected by noise. Since wind turbulence varies over time, it becomes possible to estimate the realistic parameters of wind turbines. Reference [20] used natural wind turbulence as excitation to estimate the drivetrain parameters of a fixed-speed wind turbine. Such a method is non-intrusive, and its measurements are always available. Therefore, it is a perfect complement to the post-disturbance method.

This paper extends the method in [20] by estimating the parameters of the drivetrain and pitch angle controller in a DFIG WT. The parameter estimation procedure is formulated as a nonlinear least-squares problem, and the parameters are estimated based on an improved weighted L-M optimization method, which is applicable when there is more than one dynamic mode or close modes in the system [21]. The novelty of this paper is summarized below:

(1) A simplified model related to the mechanical system of the DFIG WT is derived according to the model reduction technique. The obtained model can be used to estimate its mechanical parameters under turbulence excitations.
(2) The parameter sensitivity of Power Spectral Density (PSD) is introduced, which can be used to quantify the impacts of individual parameters on the dynamics of the mechanical system. The influential parameters are selected based on the sensitivity values.
(3) A weighted optimization problem is formulated for parameter estimation. A two-step parameter estimation process is proposed.

The rest of the paper is organized as follows. Section 2 presents the small signal stability analysis of the DFIG WT and describes simulations under turbulence excitations. Section 3 describes the sensitivity analysis technique, the parameter estimation process and the estimation results. Section 4 presents the conclusions of the paper.

2. Dynamics of the DFIG WT

2.1. Model of DFIG WT

Figure 1 illustrates the block diagram of the DFIG WT model [22], which includes modules representing the drivetrain, pitch angle controller, generator, back-to-back converter and its controller. Generally, the equivalent circuit of the DFIG is similar to that of an induction machine. The converter controller consists of rotor side control and grid side control. The rotor side control aims to control the DFIG output active power for tracking the input of the wind turbine torque and to maintain the terminal voltage at the control setting. Meanwhile, the grid side converter controller is normally utilized to maintain the *DC* link voltage and to regulate the terminal reactive power. This paper focuses on the slower dynamics associated with the drivetrain and the pitch angle controller. Accordingly, only the drivetrain and pitch angle controller are discussed in detail; other components can be found in [23].

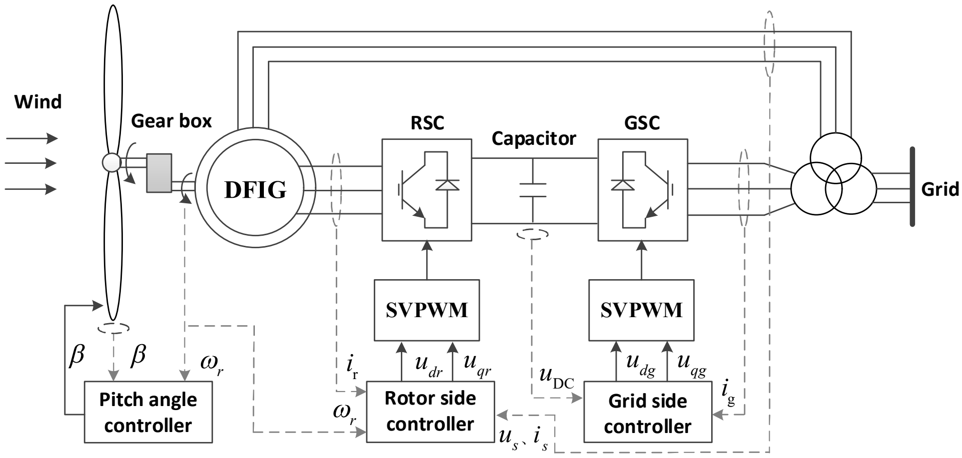

Figure 1. The block diagram of DFIG WT model.

The two-mass model of the drivetrain is defined as follows:

$$\begin{cases} \frac{d\omega_r}{dt} = \frac{T_m - K_{sh}\theta_{tw} - D_{sh}[\omega_r - (1-s_r)\omega_s]}{T_t} \\ \frac{d\theta_{tw}}{dt} = \omega_B[\omega_r - (1-s_r)\omega_s] \\ \frac{ds_r}{dt} = \frac{-T_e - K_{sh}\theta_{tw} - D_{sh}[\omega_r - (1-s_r)\omega_s]}{T_g} \end{cases} \tag{1}$$

where ω_r and θ_{tw} are the wind turbine angle speed and shaft equivalent torsional angle, respectively; T_t and T_g represent the inertia constant of the turbine and that of the generator, respectively; K_{sh} is the shaft stiffness coefficient; and D_{sh} is the damping coefficient. The electromagnetic torque T_e and mechanical torque T_m are as follows:

$$T_e = P_e/\omega_s = \left(E'_d i_{ds} + E'_q i_{qs}\right)/\omega_s \tag{2}$$

$$T_m = 0.5\rho\pi R^2 C_p v_w^3/\omega_r \tag{3}$$

where P_e is the stator active power; E'_d and E'_q are the *d*- and *q*-axis voltages behind the transient reactance, while i_{ds} and i_{qs} are the *d*- and *q*-axis stator currents; ρ is the air density; R is the wind turbine blade radius; v_w is the wind speed; and C_p is the power coefficient, the maximum value of which can be achieved by controlling the WT speed.

The pitch angle β is controlled such that the rotating speed of the WT can be maintained at the optimal speed. Figure 2 illustrates the specific control loop, and the corresponding dynamic equations are described in (4).

$$\begin{cases} dx_8/dt = \omega_{r.ref} - \omega_r \\ \beta_{ref} = K_r\left(\omega_{r.ref} - \omega_r\right) + K_r x_8/T_r \\ d\beta/dt = \left(\beta_{ref} - \beta\right)/T_\beta \end{cases} \tag{4}$$

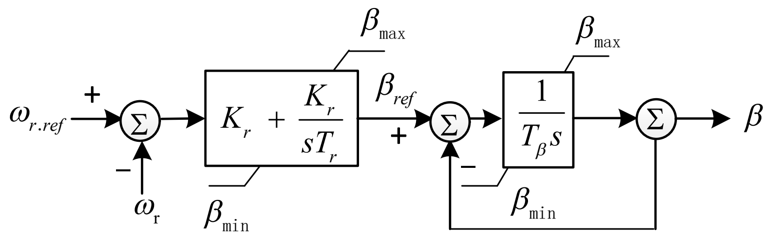

Figure 2. Pitch angle controller.

The parameters x_8, K_r and T_r denote the inner state variable, the proportional gain and the integral coefficients of the pitch angle controller, respectively; T_β denotes the time constant of the actuators, and β_{ref} and $\omega_{r\cdot ref}$ are the pitch angle and rotor speed set points.

2.2. Small Signal Stability Analysis

The dynamic characteristics of the DFIG WT can be evaluated based on the eigenvalues derived by linearizing its dynamic equations around the operating point. A single machine infinite bus (SMIB) system consisting of a wind farm with 6 DFIG wind turbines, a motor load and an infinite voltage source is used as an example in the following. The details of the system are shown in Figure 3, which can be found in MATLAB v7.1 Demo.

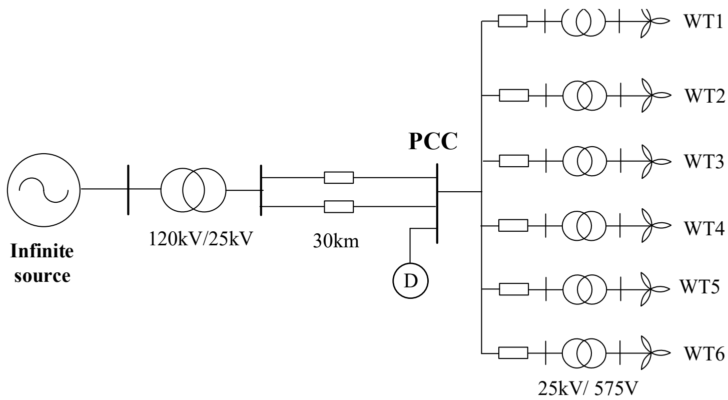

Figure 3. A SMIB system with DFIG wind farm interconnection.

Small signal stability analysis for the SMIB system was carried out, and its eigenvalues and participation factors are shown in Table 1. In Table 1, x_1~x_4 are the inner state variables of the rotor side converter controller; v_{DC} is the capacitor *DC* voltage; x_5~x_7 are the inner state variables of the grid side converter controller, and *P* is the participation factor.

Table 1. Eigenvalues and dominant participation factors.

$\lambda = \sigma \pm j\,\omega$	ζ/%	f/Hz	Dominant States and Their Participation Factors
$\lambda_{1,2} = -75.42 \pm j\,379.26$	19.50	60.36	$P\_i_{ds} = 0.62$, $P\_i_{qs} = 0.89$
$\lambda_{3,4} = -193.47 \pm j\,64.88$	94.81	10.33	$P\_E'_d = 0.85$, $P\_E'_q = 0.66$
$\lambda_{5,6} = -7.30 \pm j\,67.25$	10.79	10.70	$P\_x_1 = 0.53$, $P\_x_3 = 0.58$
$\lambda_{7,8} = -20.83 \pm j\,24.66$	64.53	3.93	$P\_v_{DC} = 0.66$, $P\_x_5 = 0.65$
$\lambda_{9,10} = -0.82 \pm j\,10.41$	7.85	1.66	$P\_\theta_{tw} = 0.51$, $P\_s_r = 0.43$
$\lambda_{11,12} = -0.07 \pm j\,0.98$	7.12	0.16	$P\_\omega_t = 0.43$, $P\_x_8 = 0.50$
$\lambda_{13,14} = -27.26 \pm j\,1.08$	99.92	0.17	$P\_x_2 = 0.54$, $P\_x_4 = 0.53$
$\lambda_{15} = -60.00$	100.00	/	$P\_x_6 = 1.00$
$\lambda_{16} = -3.33$	100.00	/	$P\_\beta = 0.92$
$\lambda_{17} = -100.00$	100.00	/	$P\_x_7 = 1.00$

It can be seen from Table 1 that the SMIB system has 7 oscillation modes and 3 decaying modes. In particular, the participation factors can describe the physical nature of the system. Specifically, the eigenvalues $\lambda_{1,2}$ and $\lambda_{3,4}$ are electrical modes associated with the DFIG stator and rotor dynamics; $\lambda_{9,10}$ and $\lambda_{11,12}$ are mechanical modes associated with the drivetrain and pitch control dynamics; and $\lambda_{5,6}$, $\lambda_{7,8}$ and $\lambda_{13,14}$ are electrical modes related to the converter and controllers.

According to the computed participation factors, the state variables i_{ds}, i_{qs}, E'_d and E'_q participate mainly in modes $\lambda_{1,2}$ and $\lambda_{3,4}$, while state variables ω_t, θ_{tw}, s_r and x_8 participate mainly in modes $\lambda_{9,10}$ and $\lambda_{11,12}$, which means that electrical modes ($\lambda_{1,2}$, $\lambda_{3,4}$) and mechanical modes ($\lambda_{9,10}$, $\lambda_{11,12}$) are loosely coupled.

2.3. Dynamic Simulations of the DFIG WT under Turbulence Excitations

Simulations were performed by utilizing a 5 min simulated turbulence series as input signals [20]. The PSD of output signals (generator angle speed ω_r, pitch angle β, DC voltage v_{DC} and stator active power P_e) for a typical wind speed of 15 m/s is shown in Figure 2.

It can be seen from Figure 2 that there are two local maxima in all output signals: one is around 0.16 Hz, which is related to the eigenfrequency of the pitch angle controller; the other is around 1.60 Hz, which corresponds to the drivetrain dynamics. The converter eigenfrequency of 10 Hz is only visible in active power P_e, while the 60 Hz stator dynamics are not visible in all output signals. Since the mechanical modes (0.16 Hz and 1.65 Hz) dominate all output signals under wind turbulence excitations, the electrical dynamics can be neglected when estimating the mechanical parameters.

2.4. Model Reduction

From Table 1 and Figure 4, it can be seen that the dynamics of the WT with DFIG span a wide time scale. Specifically, the dynamics of the pitch angle controller and the drivetrain system are quite slow, and the dynamics of the converter and DFIG are faster than the mechanical ones. This indicates that the mechanical dynamics and electrical dynamics are loosely coupled.

Since the time scales for the dynamics of the WT with DFIG are highly diversified, such systems can be analyzed with the aid of the Singular Perturbation Theory. Taking Equation (5) as an example, we have:

$$\begin{cases} \dot{\boldsymbol{x}} = f(\boldsymbol{x}, \boldsymbol{y}) \\ \boldsymbol{\varepsilon}\dot{\boldsymbol{y}} = g(\boldsymbol{x}, \boldsymbol{y}) \end{cases} \tag{5}$$

System (5) is called a fast and slow system, where $\boldsymbol{x}$ and $\boldsymbol{y}$ are its slow and fast components, respectively; $\boldsymbol{\varepsilon}$ is the small parameter vector. If we focus on the slow part, the small parameters $\boldsymbol{\varepsilon}$ are set to zero, and System (5) becomes Equation (6).

$$\begin{cases} \dot{\boldsymbol{x}} = f(\boldsymbol{x}, \boldsymbol{y}) \\ 0 = g(\boldsymbol{x}, \boldsymbol{y}) \end{cases} \tag{6}$$

For the full-order model of the WT with DFIG, the time scales of the mechanical systems are much slower than those of the electrical components, and the dynamics of the mechanical components and the electrical components are decoupled. Therefore, when the parameters of the drive system and the pitch angle controller are of interest, we can ignore the fast dynamics of the DFIG WT by setting their derivatives to zero. In this case, the dynamic equations in (1) and (4), algebraic equations of electrical systems and network equations are used to constitute the simplified model of the WT with DFIG, which is applicable when the slow dynamics of the mechanical system are of concern.

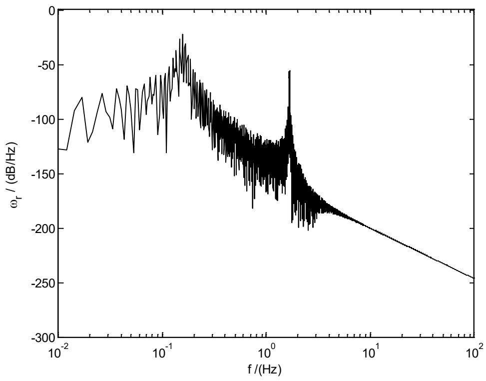

(**a**)

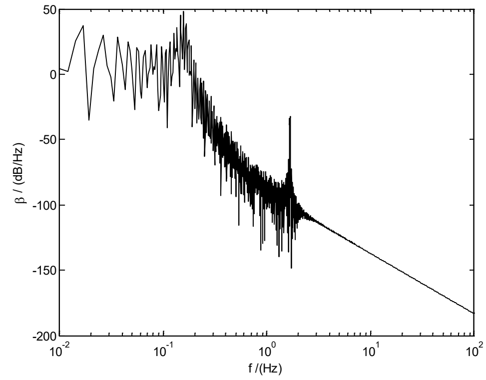

(**b**)

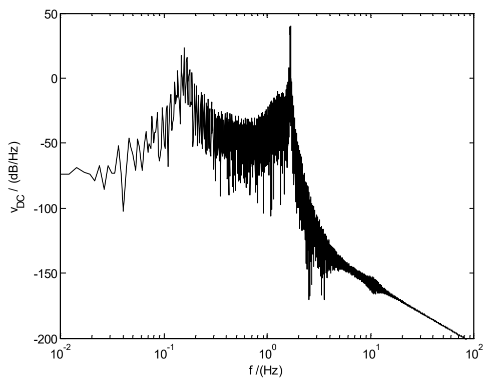

(**c**)

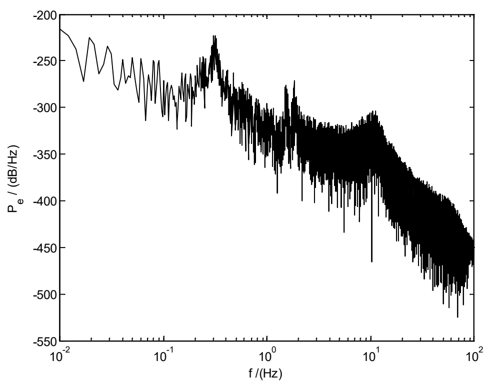

(**d**)

Figure 4. PSD of the simulated output signals. (**a**) Generator angle speed ω_r; (**b**) pitch angle β; (**c**) *DC* capacitor voltage v_{DC}; (**d**) active power P_e.

2.5. Linearization of the Simplified Model

A linear representation of the DFIG WT can be obtained around the operating condition because the magnitude of the turbulence excitations is quite small. Here, the rotor speed ω_r and pitch angle β are selected as output signals.

Linearizing Equations (2) and (3), we can respectively obtain:

$$\Delta P_e = i_{ds0}\Delta E'_d + E'_{d0}\Delta i_{ds} + i_{qs0}\Delta E'_q + E'_{q0}\Delta i_{qs} \tag{7}$$

$$\Delta T_m = a\Delta\beta + b\Delta\omega_r + c\,\Delta v \tag{8}$$

where $a = \left.\frac{\partial T_m}{\partial \beta}\right|_0$, $b = \left.\frac{\partial T_m}{\partial \omega_t}\right|_0$ and $c = \left.\frac{\partial T_m}{\partial v}\right|_0$.

Linearizing the algebraic equations of electrical systems and network equations around the operation point, we can obtain:

$$\boldsymbol{M}\Delta\boldsymbol{y} = \Delta\boldsymbol{z} \tag{9}$$

where $\Delta\boldsymbol{y}$ = $[\Delta v_{ds}, \Delta i_{ds}, \Delta i_{qs}, \Delta E'_d, \Delta E'_q, \Delta v_{dr}, \Delta v_{qr}, \Delta i_{dr}, \Delta i_{qr}]^T$, and $\Delta\boldsymbol{z}$ = $[\Delta\omega_t, \Delta s_r]^T$.

Substituting (9) into (8), we can obtain:

$$\Delta P_e = K_{pe1}\Delta\omega_t + K_{pe2}\Delta s_r \tag{10}$$

where K_{pe1} and K_{pe2} are the coefficients of $\triangle P_e$.

The linearized equations of the simplified model of the WT with DFIG are shown in (11).

$$\begin{cases} T_t\frac{d\Delta\omega_t}{dt} = (b - D_{sh})\Delta\omega_t - K_{sh}\Delta\theta_{tw} - D_{sh}\Delta s_r + a\Delta\beta + c\Delta v \\ \frac{d\Delta\theta_{tw}}{dt} = \omega_B(\Delta\omega_t + \Delta s_r) \\ T_g\frac{d\Delta s}{dt} = -(D_{sh} + K_{pe1})\Delta\omega_t - K_{sh}\Delta\theta_{tw} - (D_{sh} + k_{pe2})\Delta s_r \\ \frac{d\Delta x_8}{dt} = \Delta s_r \\ \frac{d\Delta\beta}{dt} = \frac{1}{T_\beta}K_r\Delta s_r + \frac{K_r}{T_\beta T_r}\Delta x_8 - \frac{1}{T_\beta}\Delta\beta \end{cases} \tag{11}$$

Parameters a, b and c are associated with the aerodynamic system, and they can be estimated in advance based on real measurements or identification techniques [22,24]. Once parameters a, b and c are known, the other parameters to be estimated are pitch controller parameters $\boldsymbol{\theta}_1$ = $[K_r, T_\beta, T_r]^T$ and drive system parameters $\boldsymbol{\theta}_2$ = $[T_t, T_g, K_{sh}, D_{sh}, K_{pe1}, K_{pe2}]^T$.

3. Parameter Estimation

3.1. Parameter Estimation Procedure

The simplified model of the WT with DFIG is shown in (10). When the signal of pitch angle β is used as a measurement, the parameters in $\boldsymbol{\theta_1}$ can be estimated. The transfer function from Δv to $\Delta\beta$ can be derived from Equation (11) as follows:

$$G_1(s) = \frac{\Delta\beta(s)}{\Delta v(s)} = \frac{m_2 s^2 + m_1 s + m_0}{s^5 + l_4 s^4 + l_3 s^3 + l_2 s^2 + l_1 s + l_0} \tag{12}$$

If the signal of rotor speed ω_r is used as a measurement, the parameters in $\boldsymbol{\theta_2}$ can be estimated. The transfer function from Δv to $\Delta\omega_r$ can be derived from Equation (11) as follows:

$$G_2(s) = \frac{\Delta\omega_r(s)}{\Delta v(s)} = \frac{m'_3 s^3 + m'_2 s^2 + m'_1 s}{s^5 + l_4 s^4 + l_3 s^3 + l_2 s^2 + l_1 s + l_0} \tag{13}$$

The expressions of m_0~m_2, m'_0~m'_2 and l_0~l_4 are shown in Appendix A. The parameters in $\boldsymbol{\theta_1}$ and $\boldsymbol{\theta_2}$ are estimated by the following procedure:

Step 1 Initialize the estimation of the drive system parameters $\boldsymbol{\theta_{20}}$;

Step 2 The first round of parameter estimation includes two steps: (1) estimate the pitch controller parameters in $\boldsymbol{\theta_1}$ from the power spectra of the output signal β within the frequency range for the 0.16 Hz mode; (2) on the basis of the estimated $\boldsymbol{\theta_1}$, estimate the drive system parameters in $\boldsymbol{\theta_2}$ from the power spectra of the rotor angle speed ω_r within the frequency range for the 1.66 Hz mode;

Step 3 In the second round of parameter estimation, the estimated $\boldsymbol{\theta_2}$ in the first round is used as the initial estimation, and the parameters in $\boldsymbol{\theta_1}$ and $\boldsymbol{\theta_2}$ are estimated again from the power spectra of output signals β and ω_r;

Step 4 If the error of each estimated parameter between two neighboring rounds is smaller than a small threshold value, the estimation procedure stops; otherwise, the estimation procedure returns to step 3.

3.2. Sensitivity Analysis

The impacts of parameters on system dynamics can be quantified by using the sensitivity of output power spectra, which is determined as follows.

$$S_{\theta_i} = \lim_{\Delta\theta_i \to 0} \frac{S_{YY}(\omega, \theta_1, \cdots, \theta_i + \Delta\theta_i, \cdots, \theta_m) - S_{YY}(\omega, \boldsymbol{\theta})}{\Delta\theta_i / \theta_{i0}} \tag{14}$$

where S_{θ_i} is power spectral sensitivity corresponding to parameter θ_i; θ_{i0} is the original value of θ_i; S_{YY} represents the PSD of output signal y, which can be obtained by numerical integration; Δ is the small deviation of the parameter; and m is the number of parameters to be estimated.

The influential parameters in the WT model can be identified directly based on the power spectral sensitivity. Within the frequency range of drive system dynamics, the power spectral sensitivities of parameters $\boldsymbol{\theta_2}$ = [T_t, T_g, K_{sh}, D_{sh}, K_{pe1}, K_{pe2}] are calculated; accordingly, the power spectral sensitivities of parameters $\boldsymbol{\theta_1}$ = [K_r, T_β, T_r] are computed within the frequency range of pitch angle controller dynamics. The system dynamics are more sensitive to parameters with larger sensitivity values. Therefore, the sensitivity values can be used to select important parameters to be estimated. Figure 5 and Table 2 show the power spectral sensitivities from the response data under turbulence excitation.

Table 2. PSD sensitivities of each parameter.

Module	Parameters		Sensitivity
Pitch controller t ∈ [0.05, 0.25] s	$\boldsymbol{\theta_1}$	K_r/pu	10.6048
		T_β	18.1330
		T_r	8.1299
Drive train t ∈ [1.55, 1.75]	$\boldsymbol{\theta_2}$	K_{sh}	14.8417
		D_{sh}	0.9721
		T_t	6.0793
		T_g	18.1332
		K_{pe1}	0.0678
		K_{pe2}	0.0011

It can be seen from Figure 5 and Table 2 that parameters $\boldsymbol{\theta_1}$ = [K_r, T_β, T_r] have high sensitivities around 0.16 Hz and therefore are likely to play a more important role in affecting the dynamics of the pitch angle controller system. In addition, some of the parameters in $\boldsymbol{\theta_2}$ = [T_t, T_g, K_{sh}, D_{sh}, K_{pe1}, K_{pe2}], namely, T_g, K_{sh} and T_t, have high sensitivities, while the other parameters D_{sh}, K_{pe1} and K_{pe2} have smaller effects on the drive system dynamics. In other words, parameters D_{sh}, K_{pe1} and K_{pe2} are difficult to estimate.

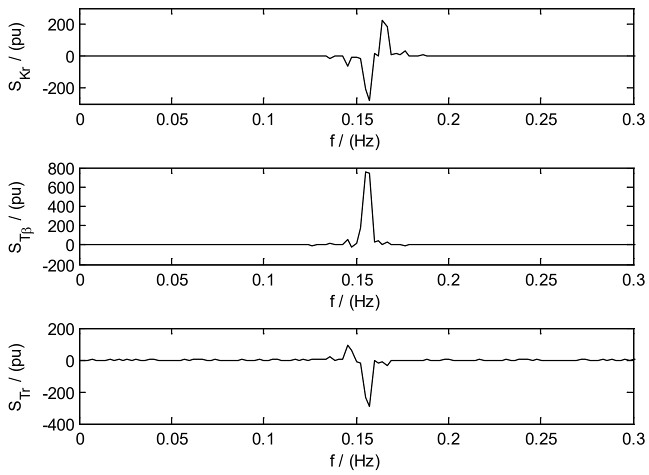

(**a**)

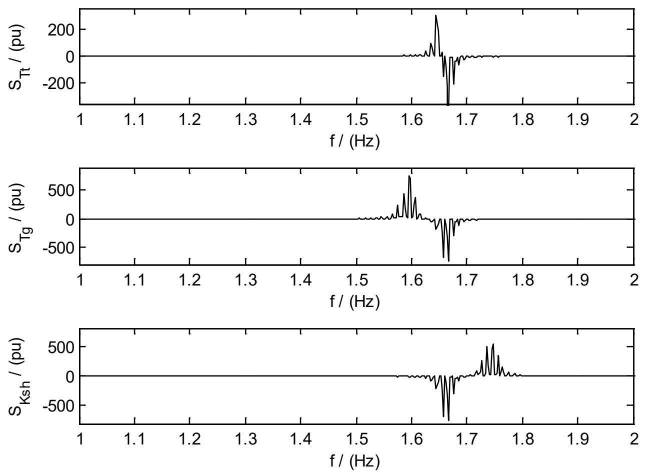

(**b**)

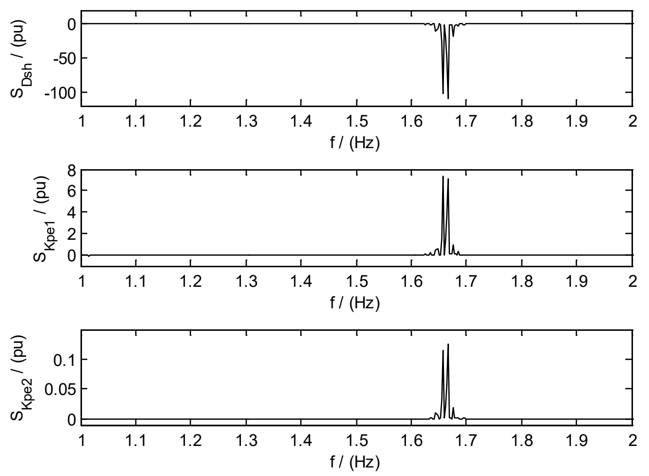

(**c**)

Figure 5. PSD sensitivity curves of each parameter. (**a**) $\boldsymbol{\theta_1}$; (**b**) T_t, T_g and K_{sh}; (**c**) D_{sh}, K_{pe1} and K_{pe2}.

3.3. Parameter Estimation with L-M Algorithm

A window size of 5 min was used to collect the measurements of β and ω_r, which yields sufficient information for parameter estimation. The objective of parameter estimation is to find the values of $\boldsymbol{\theta_1}$ = [K_r, T_β, T_r] and $\boldsymbol{\theta_2}$ = [T_t, T_g, K_{sh}, D_{sh}, K_{pe1}, K_{pe2}] such that the measured samples and the simulation trajectories are close enough to each other.

Based on the output measurement $y(t)$ and input signal $v(t)$, the measured magnitude spectrum of the transfer function can be obtained as follows:

$$|G(\omega)| = \sqrt{\frac{S_{YY}(\omega)}{S_{vv}(\omega)}} \tag{15}$$

Moreover, by replacing s with $j\omega$ in (12) and (13), the mathematical models of the magnitude spectrum are as follows:

$$\left|\hat{G}_1(j\omega)\right| = \frac{\sqrt{(m_0 - m_2\omega^2)^2 + m_1^2\omega^2}}{\sqrt{(l_4\omega^4 - l_2\omega^2 + l_0)^2 + \omega^2(\omega^4 - l_3\omega^2 + l_1)^2}} \tag{16}$$

$$\left|\hat{G}_2(j\omega)\right| = \frac{\sqrt{(m_2\omega^2)^2 + \omega^2(m_1 - m_3\omega^2)^2}}{\sqrt{(l_4\omega^4 - l_2\omega^2 + l_0)^2 + \omega^2(\omega^4 - l_3\omega^2 + l_1)^2}} \tag{17}$$

Generally, the least-squares optimization method is applied for nonlinear curve fitting. The objective function L_1 or L_2 is the difference between the measured spectrum $G(\omega)$ and the spectrum calculated from (18) or (19), which are defined as follows:

$$L_1 = \sum_{j=1}^{n}\left(|G(\omega)| - \left|\hat{G}_1\left(\omega, \hat{\theta}\right)\right|\right)^2 \tag{18}$$

$$L_2 = \sum_{j=1}^{m}\left(|G(\omega)| - \left|\hat{G}_2\left(\omega, \hat{\theta}\right)\right|\right)^2 \tag{19}$$

where n and m are the number of samples in the estimation time window.

The mode with a frequency of 0.16 Hz, which is related to pitch angle controller dynamics, dominates the output signal β, while there are two dominant oscillation modes, 0.16 Hz and 1.66 Hz, in the power spectra of the output signal ω_r. Therefore, parameters $\boldsymbol{\theta_1}$ = [K_r, T_β, T_r] are estimated first from objective function L_1, after which the parameters $\boldsymbol{\theta_2}$ = [T_t, T_g, K_{sh}, D_{sh}, K_{pe1}, K_{pe2}] are estimated from objective function L_2.

There are two dominant oscillation modes, 0.16 Hz and 1.66 Hz, in the power spectra of the output signal ω_r. The 0.16 Hz mode may affect the frequency response of the 1.66 Hz mode in the power spectrum, which may result in a large estimation error. In order to solve this problem, a weighted function [25,26] is formulated in objective function L_2, and Equation (19) is updated to the following format.

$$L_2 = \sum_{j=1}^{m} w_j\left(|G(\omega)| - \left|\hat{G}_2(\omega, \hat{\boldsymbol{\theta}})\right|\right)^2 \tag{20}$$

The weight coefficient is selected based on experience; here, we choose:

$$w_j = 1/(f - f_m) \tag{21}$$

where f_m is an eigenfrequency of 1.66 Hz.

3.4. Parameter Estimation Results

The parameter estimation results from two rounds with the L-M method are shown in Table 3.

Table 3. Estimated values in two estimation rounds.

Parameters		Real Values	L-M			PSO		
			1st Round Estimation	2nd Round Estimation	Error/%	1st Round Estimation	2nd Round Estimation	Error/%
Drive system	K_{sh}/pu	0.3	0.2765	0.2809	−6.3667	0.2654	0.2764	−7.8667
	D_{sh}/pu	0.1	0.1010	0.0999	−0.0100	0.1501	0.1138	13.8001
	T_t/s	6.0	5.3636	5.3635	−10.6083	6.7803	6.7550	12.5833
	T_g/s	1.0	0.9456	0.9446	−5.5400	0.9552	0.9637	−3.6298
	K_{pe1}/pu	−0.0523	−0.0395	−0.0396	24.2830	−0.0665	−0.0662	−26.5774
	$K_{pe2}/10^{-4}$	−1.4944	−2.0379	−2.0379	/	−0.7300	−0.7301	−51.1442
Pitch angle controller	K_r/pu	10.0	9.5355	9.5355	−4.6450	11.6203	10.5357	5.3570
	T_β/s	0.3	0.3458	0.3458	15.2667	0.2538	0.2834	−5.5333
	T_r/s	0.3	0.3484	0.3448	14.9333	0.3500	0.3210	7.0325

It can be seen from Table 3 that

(1) Parameters T_g, K_{sh} and T_t in $\boldsymbol{\theta_2}$ have larger sensitivities, and the corresponding estimation accuracies are much higher;
(2) The initial estimation of D_{sh} is quite close to its real value, indicating a good estimation accuracy, while the error of K_{pe1} and K_{pe2} makes their estimation results implausible.
(3) Additionally, the estimation results of parameters in $\boldsymbol{\theta_1}$ are in line with their sensitivity values in Table 3.

3.5. Parameter Estimation Accuracy Compared with PSO Algorithm

To validate the estimation results of the L-M method, the estimation accuracies of the particle swarm optimization (PSO) algorithm [27] are compared with those of the L-M method. PSO is an evolutionary algorithm, which is suitable for solving large-scale nonlinear optimization problems. A group of random particles are initialized first, and then the optimal solution is found through multiple iterations. In each iteration, the historical best position of the particle itself and the best position in the neighborhood are used to guide the search. The selected particles are equal to the number of estimated parameters, and the upper and lower bounds of the parameters are within the range of [−50%, 200%] relative to the real values. The parameter estimation results with the PSO method are also shown in Table 3.

It can be seen from Table 3 that most parameter estimation accuracies based on the PSO method are very close to those of the L-M method, which shows that the L-M optimization method is applicable. However, the estimation accuracies of D_{sh}, K_{pe1}, K_{pe2} and T_t remain high in both methods. The reasons are as follows:

(1) The excitation degree of wind turbulence is very small, and the system dynamics may not be fully excited; therefore, parameters are more difficult to estimate than those under fault disturbances. However, online parameter estimation is very useful in power systems because ambient data are always available, in contrast to insufficient post-disturbance data, which are only relevant when disturbances occur.
(2) Parameter estimation accuracy is related not only to sensitivity but also to the initial estimations. According to the trajectory sensitivity results in Table 2, we can see that the sensitivities of D_{sh}, K_{pe1} and K_{pe2} are very small, which shows that they are difficult to estimate. Therefore, their estimation accuracy is not desirable. The high estimation errors of parameters T_t, T_β or Tr may come from their initial estimation bias.

4. Conclusions

Simulation results demonstrate that the drive system and pitch controller dominate the dynamics of a WT with DFIG under turbulence excitations, which implies the feasibility of estimating drivetrain and pitch controller parameters by neglecting the electrical dynamics of the WT.

A sensitivity index of PSD is proposed in this paper to illustrate the difficulty of estimating parameters. The results indicate that it is much easier to estimate a parameter with a larger sensitivity.

The mechanical system parameters are successfully estimated by formulating the system as a weighted least-squares optimization problem, which is applicable when there are two or more dominant modes in output signals. The results with two types of estimation methods show that the estimated values agree well with the sensitivity values. The parameter estimation accuracy is also discussed.

Author Contributions: Software, conceptualization, formal analysis, methodology, writing—original draft preparation, investigation and data curation, X.P., J.G., D.H. and W.L.; validation, resources, writing—review and editing, supervision and project administration, X.P., J.G., Y.L. and L.Z. All authors have read and agreed to the published version of the manuscript.

Funding: This research was funded by the Science and Technology Project of the State Grid, grant number 5100-202040007A-0-0-00.

Informed Consent Statement: Not applicable.

Data Availability Statement: All materials were obtained from Reference [18] of this paper.

Conflicts of Interest: The authors declare no conflict of interest.

Appendix A

The expressions of m_0~m_2, m'_0~m'_2 and l_0~l_4 are as follows:

$$m_0 = -c\frac{\omega_0 K_r K_{sh}}{T_\beta T_g T_t T_r} \quad \text{(A1)}$$

$$m_1 = -c\frac{\left(D_{sh} + K_{pe1} + \omega_0 K_{sh} T_r\right) K_r}{T_\beta T_g T_t T_r} \quad \text{(A2)}$$

$$m_2 = -c\frac{K_r\left(D_{sh} + K_{pe1}\right)}{T_\beta T_g T_t} \quad \text{(A3)}$$

$$m'_1 = \frac{c\omega_0 K_{sh}}{T_\beta T_g T_t} \quad \text{(A4)}$$

$$m'_2 = c\frac{\left(D_{sh} + K_{pe1} + \omega_0 K_{sh} T_\beta\right)}{T_\beta T_g T_t} \quad \text{(A5)}$$

$$m'_3 = c\frac{\left(D_{sh} + K_{pe1}\right)}{T_g T_t} \quad \text{(A6)}$$

$$l_0 = \frac{\omega_0 K_r K_{sh} a}{T_\beta T_g T_r T_t} \quad \text{(A7)}$$

$$l_1 = \frac{\left(D_{sh} + K_{pe1}\right) K_r a + \omega_0 K_{sh} T_r \left(K_{pe2} - K_{pe1} - b\right)}{T_\beta T_g T_r T_t} + \frac{\omega_0 K_r K_{sh} T_r a}{T_\beta T_g T_r T_t} \quad \text{(A8)}$$

$$\begin{aligned} l_2 = {} & \frac{D_{sh} T_r \left(K_{pe2} - K_{pe1} - b\right) - K_{pe2} T_r b}{T_\beta T_g T_r T_t} + \frac{\omega_0 K_{sh} T_r \left(T_g + T_t\right) + \left(D_{sh} + K_{pe1}\right) K_r T_r a}{T_\beta T_g T_r T_t} \\ & + \frac{\omega_0 K_{sh} T_\beta T_r \left(K_{pe2} - K_{pe1} - b\right)}{T_\beta T_g T_r T_t} \end{aligned} \quad \text{(A9)}$$

$$l_3 = \frac{(D_{sh}-b)T_gT_r+\left(D_{sh}+K_{pe2}\right)T_rT_t}{T_\beta T_gT_rT_t} + \frac{\left(K_{pe2}-K_{pe1}\right)D_{sh}T_\beta T_r-\left(D_{sh}+K_{pe2}\right)T_\beta T_rb}{T_\beta T_gT_rT_t} + \frac{\omega_0K_{sh}T_\beta T_r\left(T_g+T_t\right)}{T_\beta T_gT_rT_t} \tag{A10}$$

$$l_4 = \frac{T_gT_rT_t + D_{sh}T_\beta T_r\left(T_g+T_t\right)}{T_\beta T_gT_rT_t} + \frac{K_{pe2}T_\beta T_rT_t - T_\beta T_gT_rb}{T_\beta T_gT_rT_t} \tag{A11}$$

References

1. Lorenzo-Bonache, A.; Honrubia-Escribano, A.; Jimenez-Buend, F.; Gomez-Lazaro, E. Field validation of generic type 4 wind turbine models based on IEC and WECC guidelines. *IEEE Trans. Energy Convers.* **2019**, *34*, 933–941. [CrossRef]
2. Zhang, Q.F.; He, J.H.; Xu, Y.; Hong, Z.Q.; Chen, Y.; Strunz, K. Average-value modeling of direct-driven PMSG-based wind energy conversion systems. *IEEE Trans. Energy Convers.* **2021**, *37*, 264–273. [CrossRef]
3. Asmine, M.; Brochu, J.; Fortmann, J.; Gagnon, R.; Kazachkov, Y.; Langlois, C.E.; Muljadi, E.; MacDowell, J.; Pourbeik, P. Model validation for wind turbine generator models. *IEEE Trans. Power Syst.* **2011**, *26*, 1769–1782. [CrossRef]
4. Trilla, L.; Gomis-Bellmunt, O.; Junyent-Ferré, A.; Mata, M.; Sánchez Navarro, J.; Sudrià-Andreu, A. Modeling and validation of DFIG 3-MW wind turbine using field test data of balanced and unbalanced voltage sags. *IEEE Trans. Power Syst.* **2011**, *2*, 509–519. [CrossRef]
5. González-Cagigal, M.A.; Rosendo-Macías, J.A.; Gómez-Expósito, A. Parameter estimation of wind turbines with PMSM using cubature kalman filters. *IEEE Trans. Power Syst.* **2020**, *35*, 1796–1804. [CrossRef]
6. Wang, T.; Huang, S.L.; Gao, M.Y.; Wang, Z.P. Adaptive extended kalman filter based dynamic equivalent method of PMSG wind farm cluster. *IEEE Trans. Ind. Appl.* **2021**, *57*, 2908–2917. [CrossRef]
7. Wang, P.; Zhang, Z.Y.; Huang, Q.; Wang, N.; Zhang, X.; Lee, W.J. Improved wind farm aggregated modeling method for large-scale power system stability studies. *IEEE Trans. Power Syst.* **2018**, *33*, 6332–6342. [CrossRef]
8. Jin, Y.Q.; Lu, C.J.; Ju, P.; Rehtanz, C.; Wu, F.; Pan, X.P. Probabilistic preassessment method of parameter identification accuracy with an application to identify the drive train parameters of DFIG. *IEEE Trans. Power Syst.* **2020**, *35*, 6332–6342. [CrossRef]
9. Wu, Y.K.; Zeng, J.J.; Lu, G.L.; Chau, S.W.; Chiang, Y.C. Development of an equivalent wind farm model for frequency regulation. *IEEE Trans. Ind. Appl.* **2020**, *56*, 2360–2374. [CrossRef]
10. Pedersena, J.K.; Helgelsen-Pedersena, K.O.; Poulsenb, N.K.; Akhmatovc, V.; Hejde Nielsena, A. Contribution to a dynamic wind turbine model validation from a wind farm islanding experiment. *Electr. Power Syst. Res.* **2003**, *64*, 41–51. [CrossRef]
11. Littler, T.; Fox, B.; Flynn, D. Measurement-based estimation of wind farm inertia. In Proceedings of the IEEE Conference on Power Technology, Petersburg, Russia, 27–30 June 2005; p. 5.
12. Kayikci, M.; Milanovic, J.V. Dynamic contribution of DFIG-based wind plants to system frequency disturbances. *IEEE Trans. Power Syst.* **2009**, *24*, 859–867. [CrossRef]
13. Kennedy, J.M.; Fox, B.; Littler, T.; Flynn, D. Validation of fixed speed induction generator models for inertial response using wind farm measurements. *IEEE Trans. Power Syst.* **2011**, *26*, 1454–1461. [CrossRef]
14. González-Longatt, F.; Regulski, P.; Wall, P.; Terzija, V. Fixed speed wind generator model parameter estimation using improved particle swarm optimization and system frequency disturbances. In Proceedings of the IET Conference on Renewable Power Generation, Edinburgh, UK, 6–8 July 2011; p. 6.
15. Thomsen, S.; Rothenhagen, K.; Fuchs, F. Online parameter identification methods for doubly fed induction generators. In Proceedings of the IEEE Power Electronics Specialists Conference (PESC), Rhodes, Greece, 15–19 June 2008; pp. 2735–2741.
16. Belmokhtar, K.; Ibrahim, H.; Merabet, A. Online parameter identification for a DFIG driven wind turbine generator based on recursive least squares algorithm. In Proceedings of the IEEE 28th Canadian Conference on Electrical and Computer Engineering, Halifax, NS, Canada, 3–6 May 2015; pp. 965–969.
17. Kélouwani, S.; Agbossou, K. Nonlinear model identification of wind turbine with a neural network. *IEEE Trans. Energy Convers.* **2004**, *19*, 607–612. [CrossRef]
18. Zhao, H.; Liu, H.; Hu, W.; Yan, X. Anomaly detection and fault analysis of wind turbine components based on deep learning network. *Renew. Energy* **2018**, *127*, 825–834. [CrossRef]
19. Chao, Z.; Wang, S.; Liu, Y.; Liu, C.; Xie, W.; Fang, C.; Liu, S. A novel equivalent model of active distribution networks based on LSTM. *IEEE Trans. Neural Netw. Learn. Syst.* **2019**, *30*, 2611–2624.
20. Pan, X.P.; Ju, P.; Wu, F.; Jin, Y.Q. Parameter estimation of drive system in a fixed-speed wind turbine by utilising turbulence excitations. *IET Gener. Transm. Distrib.* **2013**, *7*, 665–673. [CrossRef]
21. Ning, J.; Pan, X.P.; Venkatasubramanian, V. Oscillation modal analysis from ambient synchrophasor data using distributed frequency domain optimization. *IEEE Trans. Power Syst.* **2013**, *28*, 1960–1968. [CrossRef]
22. Sørensen, P.; Hansen, A.; Janosi, L.; Bak-Jensen, B. *Simulation of Interaction between Wind Farm and Power System*; Risø National Laboratory: Roskilde, Denmark, 2001.
23. Wu, F.; Zhang, X.P.; Godfrey, K.; Ju, P. Small signal stability analysis and optimal control of a wind turbine with doubly fed induction generator. *IET Gener. Transm. Distrib.* **2007**, *1*, 751–760. [CrossRef]

24. Monroy, A.; Alvarez-Icaza, L. Real-time identification of wind turbine rotor power coefficient. In Proceedings of the IEEE Conference on Decision & Control, San Diego, CA, USA, 13–15 December 2006; pp. 3690–3695.
25. Extending Linear Regression: Weighted Least Squares, Heteroskedasticity, Local Polynomial, Regression. Available online: https://www.stat.cmu.edu/~{}cshalizi/350/lectures/18/lecture-18.pdf (accessed on 23 October 2009).
26. Manousakis, N.M.; Korres, G.N. A weighted least squares algorithm for optimal PMU placement. *IEEE Trans. Power Syst.* **2013**, *28*, 3499–3500. [CrossRef]
27. Trelea, I. The particle swarm optimization algorithm: Convergence analysis and parameter selection. *Inf. Process. Lett.* **2003**, *85*, 317–325. [CrossRef]